

# Kinetics of alpha precipitation in Ti-6 wt % Cr and Ti-11 wt % Mo

M. UNNIKRISHNAN, E. S. K. MENON, S. BANERJEE

*Metallurgy Division, Bhabha Atomic Research Centre, Trombay, Bombay 400 085, India*

The morphology and kinetics of the precipitation of the alpha phase produced by two different heat treatment routes, namely, (a) direct isothermal decomposition and (b)  $\beta$ -quenching and subsequent ageing, were studied. In isothermally decomposed samples the  $\beta'$  (supersaturated)  $\rightarrow \alpha + \beta$  transformation was seen to occur mainly through the discontinuous growth of the transformed zone consisting of groups of parallel side plates from the grain boundary regions towards the interior of the grain. Unlike for the case of a regular discontinuous precipitation, here the transformed regions are not separated from the untransformed by an incoherent interface and the growing  $\alpha$ -plates do obey a fixed orientation relationship with the grain from which they are evolved. The theory of cellular reaction has been applied to explain the growth rate of the duplex ( $\alpha + \beta$ ) region. The overall reaction kinetics were analysed on the basis of the Johnson–Mehl formulation and were found to be consistent with that of a discontinuous precipitation reaction, where grain boundary nucleation sites were saturated at an early stage of the transformation. The structure of the  $\beta$ -quenched samples showed a uniform distribution of athermal omega particles which acted as precursors to the  $\alpha$ -precipitates. As a consequence, the reaction rate was greatly enhanced and  $\alpha$ -precipitation in the quenched and aged samples was seen to occur continuously in the entire body of the grain.

## 1. Introduction

Titanium alloys having a two-phase structure in which the  $\alpha$ -phase is distributed in a Widmanstätten pattern in the matrix of the  $\beta$ -phase have been found to exhibit an unusual combination of high strength and good fracture toughness [1–3]. Such a structure normally arises from the decomposition of the metastable  $\beta$ -phase in the ( $\alpha + \beta$ ) and  $\beta$ -titanium alloys. Phase transformations in these alloys were reviewed by McQuillon [4] and Jaffee [5] and it was shown that the precipitation of  $\alpha$  in a  $\beta$ -matrix occurs in the ( $\alpha + \beta$ )-alloys during the continuous cooling of these alloys after the hot forming or the annealing operation. In the quenched  $\beta$ -alloys, however, the high temperature  $\beta$ -phase is retained in a metastable condition and only during a subsequent ageing treatment does the  $\alpha$ -phase precipitate out. The morphology of the  $\alpha$ -precipitates in the  $\beta$ -matrix can be drastically changed by selecting one of the following heat treatment sequences. (a)  $\beta$ -quenching followed by

ageing and (b) isothermal holding in the ( $\alpha + \beta$ )-phase field subsequent to the  $\beta$ -solutionizing. It has been reported that alloys subjected to the latter treatment exhibit a strength and ductility combination and impact properties generally superior to those obtained by quenching and ageing [6]. The present work was undertaken to examine the influence of these heat treatment sequences on the morphology of  $\alpha$ -plates.

In a detailed investigation of the precipitation reaction in a hypoeutectoid Ti-7.22% Cr alloy, Aaronson *et al.* [7] concluded that  $\alpha$ -precipitation proceeds by the growth of Widmanstätten side plates and that the morphology of these precipitates can be described on the basis of Dube's classification scheme [8–11]. Aaronson [12] also measured the growth rates of isothermally precipitated  $\alpha$ -plates and compared these results with the values of the growth rates calculated from the Zener–Hillert equation. However, a detailed investigation of the kinetics of the precipitation reaction

in these alloys has not yet been attempted. In the present work, an attempt has been made to study the kinetics of the  $\alpha$ -precipitation reaction in two binary titanium alloys from metallographic observations adopting two different heat treatment sequences. It should be mentioned that the alloys Ti-6 wt% Cr and Ti-11 wt% Mo (hereafter referred to as Ti-6 Cr and Ti-11 Mo, respectively) used in this investigation belong to two different categories of alloy systems ( $\beta$ -eutectoid and  $\beta$ -isomorphous respectively). Since the precipitation of the intermetallic  $\text{TiCr}_2$  phase is very sluggish, only  $\alpha$ -precipitation occurs during the initial stages of the decomposition of the  $\beta$ -phase in this alloy [13].

## 2. Experimental

The alloys were melted in a non-consumable, tungsten electrode arc furnace in which a protective atmosphere of argon was maintained. Premelted sponge titanium, super-pure chromium (99.99% pure) and molybdenum (99.99% pure) were used for the alloy preparation. The alloys were remelted three to four times and were then hot rolled at 850–900° C to a thickness of 2 mm. The Ti-6 Cr alloy could not be rolled down to lower thicknesses, whereas the Ti-11 Mo alloy could be cold rolled to about 0.75 mm. The chemical analysis of the alloys showed that the true compositions of both the alloys were the same as the nominal compositions and that the interstitial contents of the alloys were 2300 ppm oxygen and 300 ppm nitrogen in Ti-6 Cr and 600 ppm oxygen and 80 ppm nitrogen in Ti-11 Mo. Two types of heat treatment were employed in the case of the Ti-6 Cr alloy: (a) isothermal ageing, i.e. transfer of the samples held at  $\beta$ -solutionizing temperature directly to the reaction temperature (625–765° C). For this purpose, a tandem arrangement of two horizontal furnaces was used. The samples were held at the reaction temperature for different lengths of time. (b) the samples were quenched from the  $\beta$ -solutionizing temperature (900° C) into ice cold water and subsequently aged at different temperatures (700–750° C). The second mode of heat treatment could not be adopted for the Ti-11 Mo alloy as the  $\beta$ -phase cannot be retained by quenching this alloy. All samples for heat treatment were of the size 1 cm  $\times$  1 cm and they were sealed in silica capsules in an atmosphere of pure helium gas. Samples for metallographic examination were mounted and polished by conventional techniques.

The etchant used was a solution containing 25 ml HF, 25 ml  $\text{HNO}_3$  and 50 ml water. Volume fraction determinations of the  $\alpha$ -phase were carried out by a point counting method [14], using a Swift Automatic Counter. Large areas of the sample were examined in order to minimize the errors.

## 3. Results and discussion

### 3.1. Morphology of isothermally treated samples

The essential features of the morphology of the precipitates observed in “isothermally treated” Ti-6 Cr and Ti-11 Mo samples were similar to those observed by Aaronson *et al.* [7] in a Ti-7.22% Cr alloy. Hence a detailed description of the morphology is not included in this paper. However, the salient features of the morphological observations are briefly mentioned.

#### 3.1.1. Ti-6 Cr

3.1.1.1. 765° C and 725° C. At these temperatures, grain boundary allotriomorphs were the first to appear. Subsequently, the reaction was observed to proceed mainly through the formation and edgewise growth of side plates (Fig. 1a). It must be emphasized that the growth of a single isolated plate was never observed. Instead, one found the growth of a group of parallel side plates in a cooperative manner. Since the nucleation of these side plates occurred only at the grain boundaries, (either on allotriomorphs or on the grain boundary itself) the reaction essentially progressed by the movement of the transformation front from the grain boundary to the interior of the grain. From this aspect, the transformation is quite similar to a discontinuous reaction [15]. However, this reaction cannot strictly be classified as a regular discontinuous reaction mainly because the transformed and untransformed regions are not separated by a well defined incoherent interface.

3.1.1.2. 675° C. At this temperature also, the reaction proceeded by the growth of the product slabs from the grain boundary to the core (Fig. 1b). The individual phases within the transformed zone could not be resolved in the optical microscope.

3.1.1.3 625° C. Though this reaction temperature was below the eutectoid temperature, within the first 10 min of the reaction only the  $\alpha$ -phase was

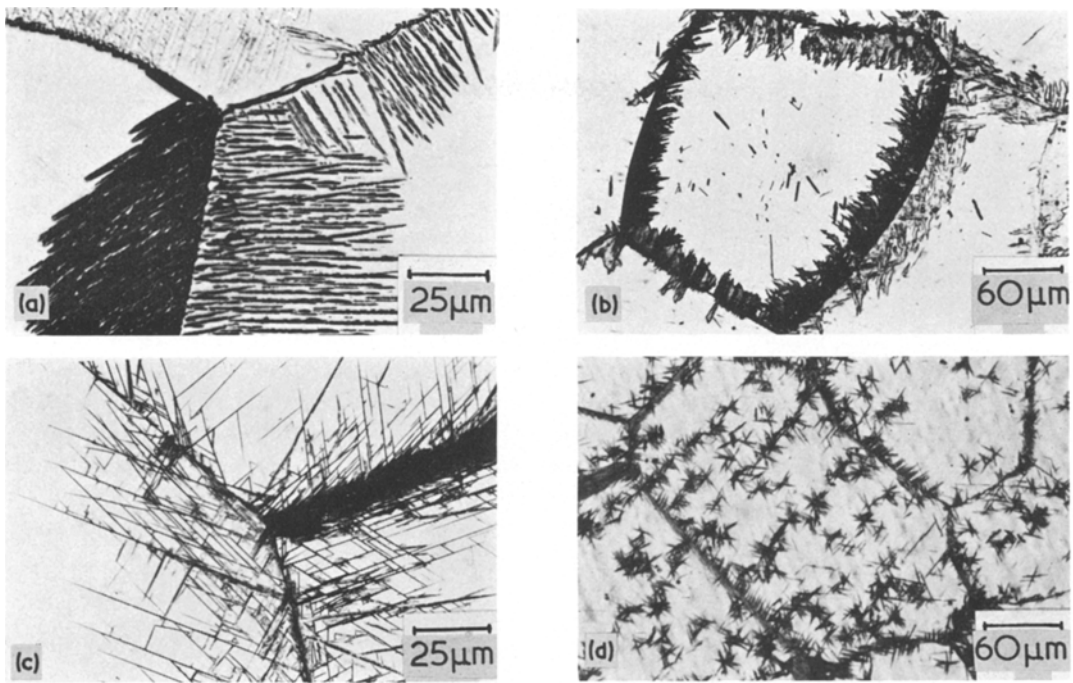


*Figure 1* (a) Ti-6 Cr, isothermally transformed at 725° C for 20 min. Groups of parallel Widmanstätten plates are seen. (b) Ti-6 Cr, isothermally transformed at 675° C for 5 min. The micrograph shows slabs of the transformed region advancing from the grain boundaries to the interior of the grain. (c) Ti-6 Cr, isothermally transformed at 625° C for 2.5 min. The martensite-like morphology is characteristic of a process involving an autocatalytic nucleation and continuous partitioning of the parent grains. (d) Ti-11 Mo, isothermally transformed at 700° C for 10 min. A large number of Widmanstätten stars are seen to be nucleated within the grains.

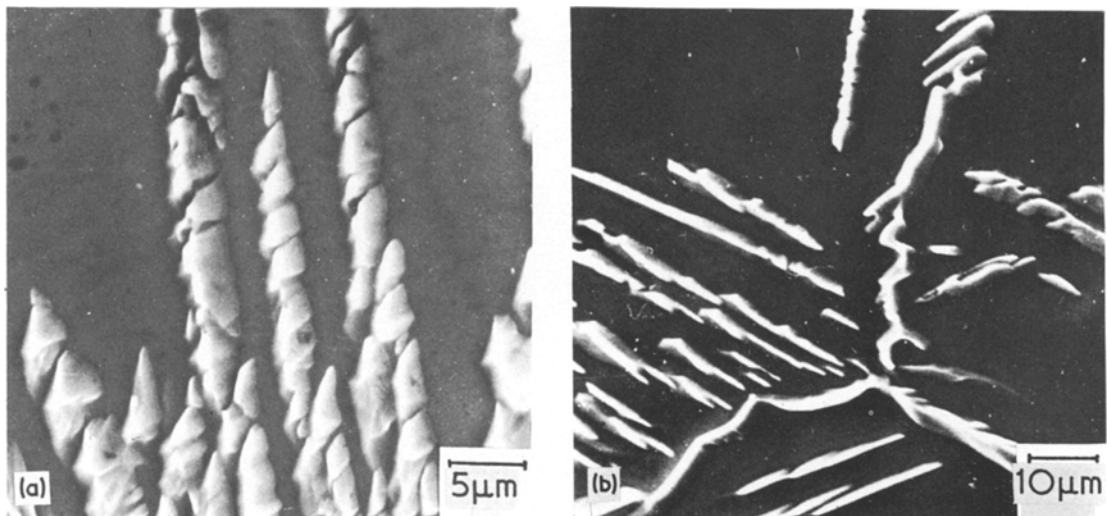


*Figure 2* SEM taken from a deep etched sample of the Ti-6 Cr alloy isothermally transformed at 750° C for 30 min. (a) Discontinuities within  $\alpha$ -plates are seen. (b) Micrograph shows degeneracies of intragranular side plates and grain boundary allotriomorphs.

seen to be precipitated out. At this temperature, side plates having very large aspect ratios were found to predominate in the structure (Fig. 1c). These plates which continuously partition the parent  $\beta$ -grains have a remarkable resemblance with martensite plates in titanium alloys. These plates were often seen to be arranged in a triangular pattern in a manner similar to the arrangement of martensite plates on  $\{3\ 3\ 4\}$  or  $\{3\ 4\ 4\}$  habit planes [16] in various titanium alloys. However, these could be clearly distinguished from martensite plates as the former did not span across the entire width of the grain. The presence of similar plates has been noticed earlier in a Ti–7.22% Cr alloy isothermally treated at 600° C, and these have been termed ‘black plates’ [7].

### 3.1.2. Ti–11 Mo

It was found that the morphology of  $\alpha$ -plates and the mode of transformation of this alloy at 750° C was in no way different from those observed in the Ti–6 Cr alloy reacted at 765° C and 725° C (compare with Figs. 1a and 1b). However, in the samples reacted at 700° C, a number of Widmanstatten stars appeared within the grains after a few minutes of the initiation of the transformation (Fig. 1d). Consequently, the growth of the transformed zone occurred not only from the grain boundary sites but also from these “stars”.

Aaronson [11] has pointed out that the Widmanstatten side plates formed at high temperatures in hypoeutectoid plain carbon steels and in Ti–Cr alloys show a significant degree of imperfections. Such degeneracies of the  $\alpha$ -plates formed in Ti–Cr and Ti–Mo alloys have been clearly resolved in the secondary electron images obtained in a scanning electron microscope shown in Figs. 2a and 2b. It was noticed that the degeneracy tended to disappear at lower temperatures and the  $\alpha$ -plates precipitated at 625° C appeared perfect. These observations suggest that each plate is not a single crystal but is made up of a continuous array of short segments of crystals of nearly identical orientations. This would imply that the edgewise growth of a plate took place by fresh nucleation of precipitate crystals at the edge of previously formed crystals of the same phase. The occurrence of such sympathetic nucleation is not favourable from the point of view of the chemical free energy change because the  $\beta$ -phase in the immediate vicinity of the growing  $\alpha$ -plate will be highly supersaturated with  $\beta$ -stabilizing solute atoms. But surface energy

requirements render the nucleation of  $\alpha$  at the  $\alpha$ – $\alpha$  interface competitive with its nucleation at the  $\alpha$ – $\beta$  interface, provided the specific energy of the  $\alpha$ – $\alpha$  interface is lower than that of the  $\alpha$ – $\beta$  interface [17].

### 3.2. Morphology of quenched and aged samples

In contrast to the discontinuous nature of  $\alpha$ -precipitation initiating from the grain boundary in isothermally transformed samples, the nucleation of  $\alpha$ -plates in quenched and aged samples was found to occur uniformly all over the grain body (Figs. 3a and b) when the decomposition reactions were carried out in the same temperature ranges. This implies that the structural changes produced by prior quenching treatment is responsible for bringing about a transition in the nature of the

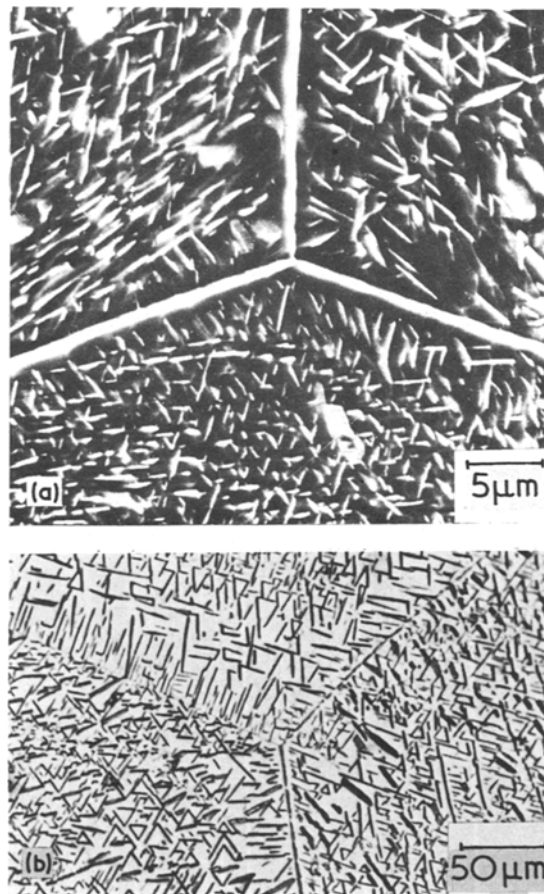


Figure 3 (a) Ti–6 Cr,  $\beta$ -quenched and subsequently aged at 750° C for 10 min. SEM shows a uniform distribution of  $\alpha$ -plates within the grains and bands of  $\alpha$  along the  $\beta$ -grain boundaries. (b) The optical micrograph of the same alloy aged for 30 min.

precipitation reaction. It was reported that  $\beta$ -quenching of Ti-6 Cr gave rise to the formation of  $\omega$ -phase [16, 18]. This was confirmed in the present work by X-ray diffraction. On ageing at 350° C these  $\omega$ -particles grew in size and it was possible to image these particles in dark field. These  $\omega$ -particles act as the embryos for the nucleation of  $\alpha$ -plates in the quenched and aged samples.

### 3.3. Kinetics

#### 3.3.1. Isothermally treated samples

It has been pointed out in the preceding section that during an "isothermal treatment", the transformation proceeds mainly through the edgewise growth of the side plates. The growth kinetics of the isothermal  $\alpha$ -phase precipitating from the supersaturated  $\beta$ -phase have been studied by Aaronson [12] by measuring the rates of lengthening of these  $\alpha$ -side plates at various reaction temperatures. He used the Zener-Hillert equation [19] for the rate of lengthening,  $G_1$ , of the precipitate plates:

$$G_1 = \frac{D(C_{\beta}^{\alpha} - C_{\beta})}{4r(C_{\beta}^{\alpha} - C_{\alpha})} \quad (1)$$

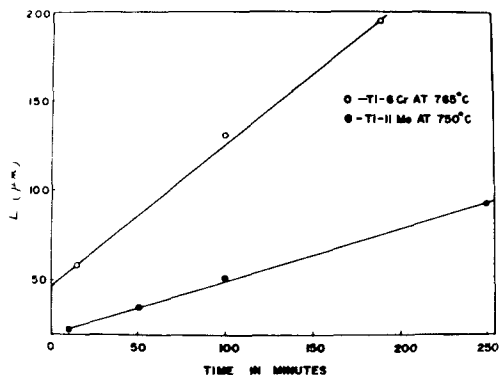


Figure 4  $L$ , the length of the longest plate has been plotted against the length of the time  $t$ , for which the samples have been held at the indicated temperatures. The slope of these linear plots gives the growth rate of the plates.

TABLE I Comparison of calculated and measured growth rates

Alloy	Tip Radius, $r$ (cm)	Spacing, $d$ (cm)	Growth Rate (cm sec <sup>-1</sup> )		
			Measured	Calculated from Equation 1	Calculated from Equation 2
Ti-6 Cr Isothermally reacted at 765° C	$2.50 \times 10^{-5}$	$5.56 \times 10^{-4}$	$1.28 \times 10^{-6}$	$2.80 \times 10^{-6}$	$1.01 \times 10^{-6}$
Ti-11 Mo Isothermally treated at 750° C	$1.50 \times 10^{-5}$	$1.80 \times 10^{-4}$	$5.00 \times 10^{-6}$	$3.00 \times 10^{-6}$	$2.00 \times 10^{-6}$

where

$D$  is the diffusivity of solute atoms in  $\beta$ -titanium  
 $C_{\beta}^{\alpha}$  is the solute content of  $\beta$  at the  $\beta$ - $\alpha$  boundary

$C_{\beta}$  is the solute content of the  $\beta$ -matrix prior to transformation

$C_{\alpha}$  is the solute content of the  $\alpha$ -phase

and  $r$  is the radius of curvature of tip of the most rapidly lengthening plate.

It has been reported [12] that the  $\alpha$ -plates in a Ti-10 Cr alloy lengthen at rates five to ten times faster than the calculated rate. Aaronson has proposed that the errors in the measurements of the tip radii and the limited accuracy of the diffusivity data are responsible for this discrepancy.

An attempt was made in the present investigation to verify whether the Zener-Hillert equation predicts a value for the growth rate consistent with the one experimentally observed. For this purpose, the length of the longest plate produced at various intervals of time,  $t$ , was plotted against time (Fig. 4). Such plots could be obtained only in the following two cases,

(a) Ti-6 Cr isothermally treated at 765° C

(b) Ti-11 Mo isothermally treated at 750° C

where the thickness of the  $\alpha$ -plates and the spacings between them were large enough for easy resolution under the optical microscope.

The average radii of the tips of these plates, the measured growth rate and the growth rate calculated from Equation 1 using the diffusivity data reported in literature [20-22] are presented in Table I.

The main difficulty in making use of the Zener-Hillert model in explaining the growth kinetics of  $\alpha$ -plates in these binary titanium alloys lies in the fact that in this model, one essentially considers the edgewise growth of a single isolated plate. In reality, however, as noted in the present case, the growth of the transformed zone occurs by the

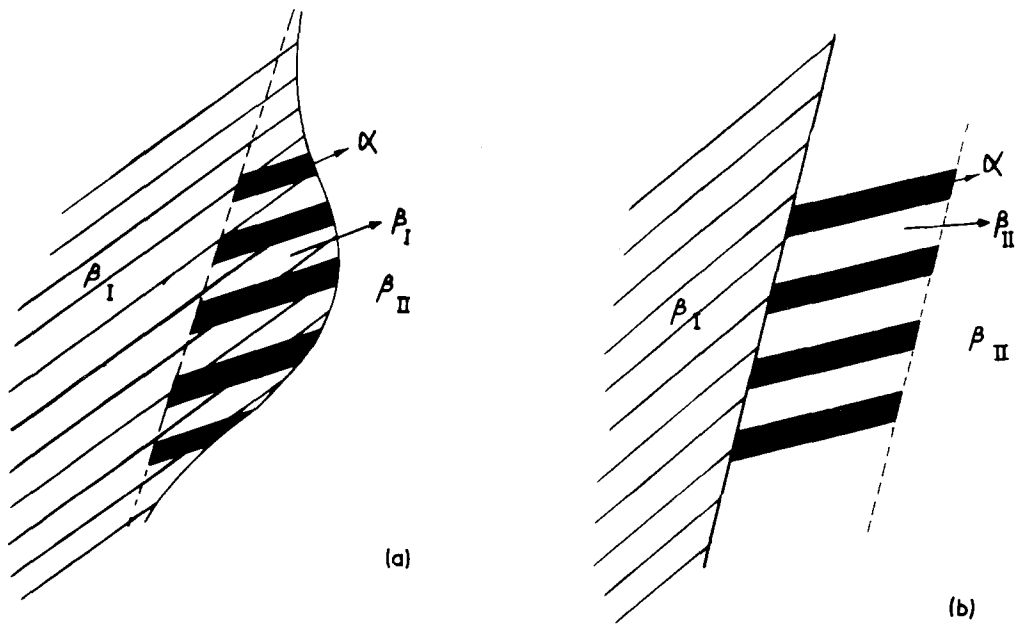


Figure 5 The difference in the orientation relationships of the precipitate phase (a) in a normal discontinuous mode of precipitation and (b) in the Ti-alloys studied here (schematic).  $\beta_I$  and  $\beta_{II}$  represent two grains of the parent phase.

simultaneous advancement of the tips of parallel  $\alpha$ -plates belonging to a group. One might consider an imaginary surface joining these tips to be the transformation front and visualize the transformation to be a discontinuous precipitation reaction. However, the characteristics of the precipitation reaction in these titanium alloys are not the same as those of a regular discontinuous precipitation. The basic differences between the two are illustrated in Fig. 5. In a regular discontinuous precipitation, the  $\alpha$ -plates which have a definite orientation relationship with the grain  $\beta_I$  grow into the  $\beta_{II}$  grain, (Fig. 5a) whereas, the  $\alpha$ -plates in the alloys studied here have a fixed orientation relationship with the  $\beta$  grain in which they grow ( $\beta_{II}$ , as shown in Fig. 5b). Consequently, the transformed and untransformed regions in the present case are not separated by any physical interface.

Despite these differences between a regular discontinuous precipitation reaction and the  $\beta' \rightarrow \alpha + \beta$  reaction in the Ti-6 Cr and Ti-11 Mo alloys, it is attractive to consider whether the theory of the kinetics of cellular reactions is applicable to this case. It should be emphasized that unlike the growth of a single plate considered in the Zener-Hillert model, the diffusion gradient associated with the growth of a duplex ( $\alpha + \beta$ ) region is mainly along a direction perpendicular to the growth

direction. Then the growth can be expressed [23] as:

$$G_1 = \frac{D(C_\beta^{\beta\alpha} - C_\beta)}{\alpha d(C_\beta^{\beta\alpha} - C_\alpha)} \quad (2)$$

where  $\alpha d$  is the diffusion distance.

The growth rates so calculated from the measured values of the interlamellar spacing  $d$ , and assuming  $\alpha \approx 0.5$ , are also presented in Table I. It can be seen from this table that the overall kinetics of this reaction agree fairly well with both the models described earlier. However, the growth morphology indicates that the advancement of the reaction front occurs by the co-operative growth of a group of  $\alpha$ -plates rather than the growth of isolated  $\alpha$ -plates. In view of this, application of the theory of cellular precipitation is considered more appropriate. In order to test whether the  $\beta' \rightarrow \alpha + \beta$  reaction in the alloys studied here could be classified as a linear one, the distance through which the transformation front advanced was plotted against the reaction time,  $t$  (Fig. 6). The straight line plots obtained corresponding to various reaction temperatures implied constant growth rates, characteristic of a linear transformation. This suggested that the compositional redistribution within the matrix did not occur continuously and that the partitioning of solute atoms in the product phases took

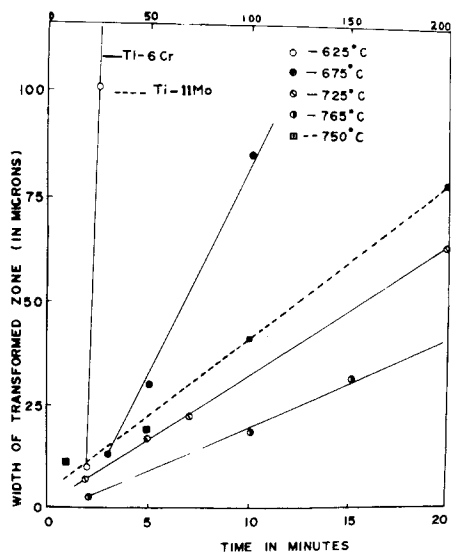


Figure 6 The width of the transformed zone plotted against the reaction time. The time axis for the Ti-11 Mo alloy is indicated at the top of the plot.

place only in the immediate vicinity of the advancing reaction front. In other words, the diffusion geometry ahead of the reaction front was presumably similar to that obtained in a regular discontinuous precipitation. Hence, by applying the theory of cellular growth to this precipitation reaction, the overall kinetics of the process can be evaluated and the various morphologies explained.

The isothermal transformation kinetics of the Ti-6 Cr and Ti-11 Mo alloys were studied by determining the volume fraction transformed as a

function of time for different temperatures. A rate equation governing the overall formation of a duplex product in a discontinuous precipitation reaction has been derived by Johnson and Mehl [24] and a generalized form of such a relation can be expressed as:

$$y = 1 - \exp [-Kt^n] \quad (3)$$

where  $y$  represents the volume fraction transformed at time  $t$ , and  $K$  and  $n$  are constants.

The kinetic data obtained in the present investigation were analysed on the basis of this Johnson-Mehl equation and are shown in Fig. 7. Considering the slope of these straight line plots which gives the value of  $n$  in Equation 3, one can classify the isothermal transformation behaviour of the Ti-6 Cr alloy into two categories.

At higher temperatures ( $\geq 675^\circ\text{C}$ ), the values of  $n$  in Equation 3 were found to be approximately equal to unity, while the slope of the plot corresponding to  $625^\circ\text{C}$  was about 4. According to theoretical calculations made by Cahn [25],  $n = 1$  corresponds to a situation where the transformation product nucleates on the grain boundary surface and the available nucleation sites soon become saturated. This is in complete agreement with the metallographic observations already discussed. One can also note from the photomicrographs presented that the product cells at the grain boundaries of the matrix coalesce into slabs, particularly at  $675^\circ\text{C}$ , and the transformation occurs mainly by the advancement of these slabs towards the centre of the grain. In order to substantiate the prop-

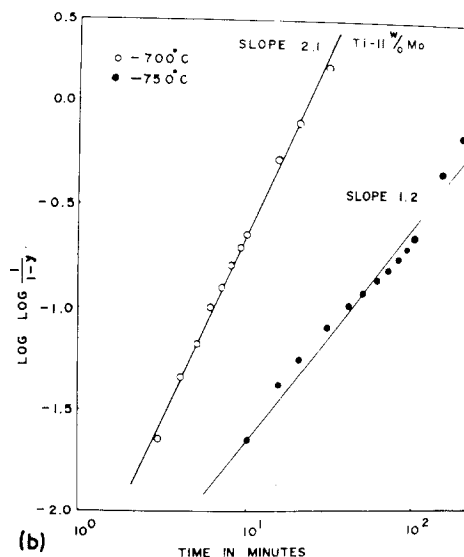
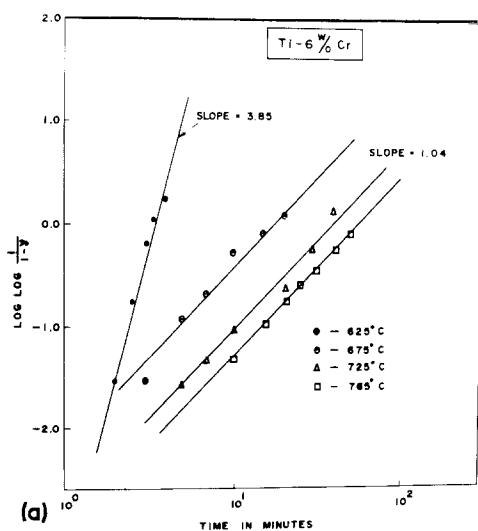


Figure 7 Johnson-Mehl plots for the two alloys reacted isothermally at the temperatures indicated.

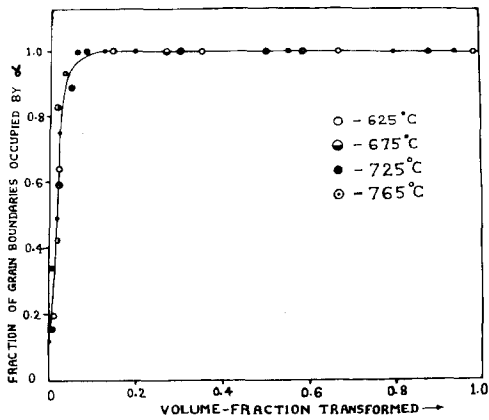


Figure 8 The fraction of the grain boundary occupied by transformed product plotted against the fraction transformed at various temperatures for the Ti-6 Cr alloy.

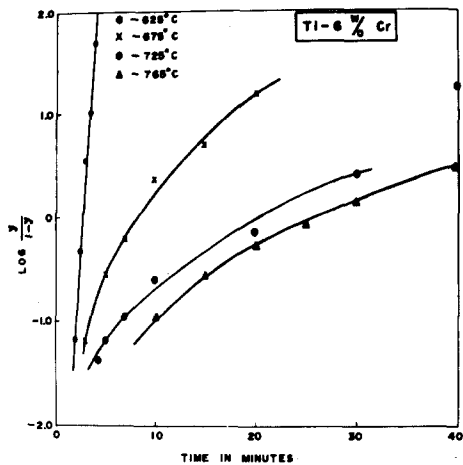


Figure 9 The linear nature of the plot of  $\log [y/(1-y)]$  versus time at  $625^\circ\text{C}$  for the Ti-6 Cr alloy suggests that the reaction proceeded autocatalytically at this temperature. This was not true for the higher reaction temperature.

osition that site saturation takes place during the early stages of the transformation, the fraction of the grain boundary occupied by the product region was plotted as a function of  $y$  for various reaction temperatures (Fig. 8). It could be seen from these plots that for  $y \geq 0.1$  all boundaries become fully occupied with continuous slabs of the reaction product. As a consequence of the early site saturation in a pearlitic or cellular precipitation reaction, the growing slabs from the grain boundaries, in general, impinge on each other. Under this condition, the growing cells never get an opportunity to cross the grain boundaries. It should be emphasized here that in the present case of  $\alpha$ -precipitation in a  $\beta$ -matrix, a product region could never cross a

grain boundary, as this would violate the orientation relationship between the  $\alpha$ -precipitates and the  $\beta$ -matrix.

The value of the exponent in Equation 3 was found to be close to 4 for the Ti-6 Cr alloy isothermally reacted at  $625^\circ\text{C}$ . According to Cahn [25], this corresponds to a situation where the nucleation rate is more or less constant. Metallographic examination of the samples treated at  $625^\circ\text{C}$  indicated that the  $\alpha$ -plates were remarkably similar in appearance to the martensite plates. Even the nature of aggregation of these plates suggested that autocatalytic nucleation occurred in this case. For an autocatalytic reaction the rate is given by [23]

$$\frac{dy}{dt} = ky(1-y). \quad (4)$$

The applicability of Equation 4 is tested by plotting  $\log [y/(1-y)]$  against  $t$ . Fig. 9 shows that the data corresponding to the transformation curve at  $625^\circ\text{C}$  could be fitted to a straight line, thus confirming the autocatalytic nature of nucleation in this case.

Kinetic data obtained from the overall reaction in the Ti-6 Cr alloy were analysed on the basis of an Arrhenius-type equation and the plot is shown in Fig. 10. The value of activation energy calculated from the slope of this plot was found to be 41.45

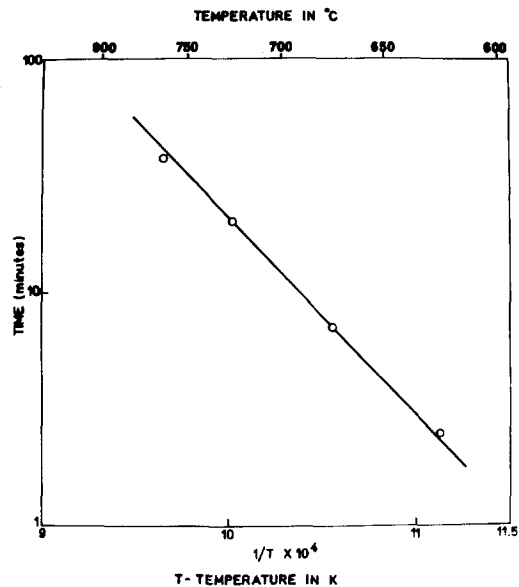


Figure 10 Plot of the time required for 50% transformation in the Ti-6 Cr alloy against the reciprocal of absolute temperature. The slope of this linear plot gave the value of the activation energy for the reaction.



kcal mole<sup>-1</sup>. This value is quite close to the activation energy (40.0 kcal mole<sup>-1</sup>) for diffusion of Cr in  $\beta$ -Ti [20, 21]. This suggests that the rate-controlling step in the reaction is the bulk diffusion of Cr in the matrix. This is in sharp contrast to what is normally encountered in a regular discontinuous precipitation reaction. In the latter case diffusion normally occurs along the advancing interface which separates the transformed volume from the untransformed matrix. Such a short-circuit diffusion is not possible in the case of the  $\beta' \rightarrow \alpha + \beta$  transformation in Ti-Cr alloys because the  $\beta$ -lamellae in the product are not separated from the  $\beta$ -matrix by any interface.

The value of the exponent  $n$  in Equation 3 was found to be close to unity for the Ti-Mo alloy isothermally reacted at 750°C. The similarity between the Ti-6 Cr alloy reacted at 765°C and 725°C and the Ti-11 Mo alloy reacted at 750°C has already been discussed. The kinetics of this alloy thus also follows the same mechanism as discussed already, namely, grain boundary nucleation followed by a discontinuous growth of the transformed zone. Metallographic observations revealed that at 700°C, some intragranular  $\alpha$  nuclei become operative and a considerable amount of  $\alpha$ -phase originated from such intragranular nucleation sites. As a consequence, the kinetics of the formation of the  $\alpha$ -phase were observed to be much faster. This was reflected in a higher value of  $n$  ( $= 2$ ) in this case.

### 3.3.2. Quenched and aged samples

The kinetics of the  $\alpha$ -precipitation in the samples water quenched from the  $\beta$ -solutionizing temperature and subsequently aged at the reaction temperatures were found to be much faster than those in the case of the samples taken directly to the reaction temperature from the  $\beta$ -solutionizing temperature. The accelerated precipitation of the  $\alpha$ -phase in the samples quenched prior to ageing can be seen qualitatively from Fig. 3a. In fact, the kinetics of the reaction were so fast that it was not possible to make any quantitative measurement on these samples. The non-chemical free energy requirement for the  $\alpha$ -precipitation within the bulk of the matrix was presumably reduced at the heterogeneities provided by the  $\omega$ -particles formed while quenching these samples, and hence nucleation throughout the grains was made easier. This would also increase the rate of nucleation and consequently the rate of the overall reaction.

## 4. Conclusions

(a) The precipitation reaction in isothermally treated samples of Ti-6 Cr and Ti-11 Mo alloys is similar to that of a discontinuous precipitation reaction. However, the product phase maintains an orientation relationship with the consumed matrix and the transformed and untransformed regions are not separated by an interface.

(b) The reaction tended to be autocatalytic at a low reaction temperature (625°C) in the Ti-6 Cr alloy, resulting in a higher growth rate. Intragranular nucleation of  $\alpha$ -plates, in addition to the normal grain boundary nucleation was responsible for the enhancement of the growth rate in the Ti-11 Mo alloy isothermally reacted at 700°C.

(c) In contrast to the case of a normal discontinuous reaction, where interfacial diffusion is the rate-controlling process, bulk diffusion was found to be rate controlling in the present case.

(d) In contrast to the isothermally treated samples,  $\alpha$ -precipitation in the quenched and aged samples of Ti-6 Cr was found to occur in a continuous manner and the reaction rate was greatly enhanced. These could be attributed to the presence of  $\omega$ -particles in the as-quenched alloy.

## Acknowledgements

The authors are thankful to Dr M. K. Asundi and Dr R. Krishnan for many helpful discussions. They also wish to express their gratitude to Mr P. Mukhopadhyay for carefully going through the manuscript. The authors gratefully acknowledge the encouragement received from Dr. V. K. Moorthy, Head, Metallurgy Group, Bhabha Atomic Research Centre.

## References

1. H. MARGOLIN and W. F. KIRK, Technical Report No. 3, WAL 401/272 (August, 1958).
2. P. A. FARRAR and H. MARGOLIN, Technical Report, WAL TR 401/303-13 (September, 1967).
3. D. B. HUNTER and S. V. ARNOLD, "The Science, Technology and Application of Titanium", edited by R. I. Jaffee and N. E. Promisel (Pergamon Press, Oxford, 1970) p. 959.
4. M. K. MCQUILLAN, *Met. Rev.* 8 (1963) 41.
5. R. I. JAFFEE, *Prog. Met. Phys.* 7 (1958) 65.
6. D. J. DE LAZARO and W. ROSTOKER, *Trans. ASM* 46 (1954) 292.
7. H. I. AARONSON, W. B. TRIPLETT and G. M. ANDES, *J. Metals* 9 (1957) 1227.
8. C. A. DUBÉ, H. I. AARONSON and R. F. MEHL, *Rev. Met.* 55 (1958) 201.
9. R. W. HECKEL and H. W. PAXTON, *Trans. ASM* 53 (1961) 539.

10. H. I. AARONSON, Symposium on the Mechanism of Phase Transformations in Metals, Institute of Metals, London (1955) p. 47.
11. *Idem*, "Decomposition of Austenite by Diffusional Processes", edited by V. F. Zackay and H. I. Aaronson (Interscience Publishers, New York, 1962). p. 387.
12. *Idem*, *Trans. Met. Soc. AIME* **224** (1962) 693.
13. POL. DUWEZ and J. L. TAYLOR, *Trans. ASM* **44** (1952) 495.
14. R. T. DE HOFF and F. N. RHINES, "Quantitative Microscopy", (McGraw-Hill, New York, 1968) p. 52.
15. J. W. CHRISTIAN, "The Theory of Transformations in Metals and Alloys", (Pergamon Press, Oxford, 1965) p. 644.
16. J. C. WILLIAMS, "Titanium Science and Technology", edited by R. I. Jaffee and H. M. Burte (Plenum Press, New York, 1973) p. 1433.
17. W. T. READ, Jr., and W. SHOCKLEY, *Phys. Rev.* **78** (1950) 275.
18. A. E. AUSTIN and J. R. DOIG, *J. Metals* **9** (1957) 27.
19. C. ZENER, *Trans. AIME* **167** (1946) 550.
20. R. F. PEART and D. H. TOMLIN, *J. Phys. Chem. Solids* **23** (1962) 1169.
21. A. J. MORTLOCK and D. H. TOMLIN, *Phil. Mag.* **4** (1959) 628.
22. R. P. ELLIOT, U.S. Report AD-290336 (March, 1962).
23. J. BURKE, "The Kinetics of Phase Transformations in Metals", (Pergamon Press, Oxford, 1965) p. 161.
24. W. A. JOHNSON and R. F. MEHL, *Trans. Amer. Inst. Min (Metall) Engrs.* **135** (1939) 416.
25. J. W. CAHN, *Acta Met.* **4** (1956) 449.

Received 27 June and accepted 17 October 1977.